星形成ゼミ 2018/3/2

SFN #301 50-52, #302 1-5

崔仁士

301

50 Spatially associated clump populations in Rosette from CO and dust maps

Todor V. Veltchev[1,2], Volker Ossenkopf-Okada[3], Orlin Stanchev[1], Nicola Schneider[3], Sava Donkov[4], and Ralf S. Klessen[2]

51 The Taurus Boundary of Stellar/Substellar (TBOSS) Survey II. Disk Masses from ALMA Continuum Observations

K. Ward-Duong[1], J. Patience[1], J. Bulger[2,3], G. van der Plas[4,5,6], F. Ménard[6], C. Pinte[6], A.P. Jackson[7,1], G. Bryden[8], N.J. Turner[8], P. Harvey[9], A. Hales[10,11], R.J. De Rosa[12]

52 Radiation Transfer of Models of Massive Star Formation. IV. The Model Grid and Spectral Energy Distribution Fitting

Yichen Zhang[1] and Jonathan C. Tan[2,3]

302

1 Similar complex kinematics within two massive, filamentary infrared dark clouds

A.T. Barnes[1,2,3], J.D. Henshaw[4], P. Caselli[3], I. Jiménez-Serra[5], J.C. Tan[6], F. Fontani[7], A. Pon[8], and S. Ragan[9]

2 On the diversity and statistical properties of protostellar discs

Matthew R. Bate[1]

3 Magnetic fields at the onset of high-mass star formation

Henrik Beuther[1], Juan Soler[1], Wouter Vlemmigs[2], Hendrik Linz[1], Thomas Henning[1], Rolf Kuiper[3], Ram Rao[4], Rowan Smith[5], Takeshi Sakai[6], Katharine Johnston[7], Andrew Walsh[8] and Siyi Feng[9]

4 K2 reveals pulsed accretion driven by the 2 Myr old hot Jupiter CI Tau b

Lauren I. Biddle[1,2], Christopher M. Johns-Krull[3], Joe Llama[1], Lisa Prato[1], and Brian A. Skiff[1]

5 Pebble isolation mass — scaling law and implications for the formation of super-Earths and gas giants

Bertram Bitsch[1], Alessandro Morbidelli[2], Anders Johansen[1], Elena Lega[2], Michiel Lambrechts[1], and Aurélien Crida[2,3]

#51 **The Taurus Boundary of Stellar/Substellar (TBOSS) Survey II. Disk Masses from ALMA Continuum Observations**

K. Ward-Duong[1], J. Patience[1], J. Bulger[2,3], G. van der Plas[4,5,6], F. Ménard[6], C. Pinte[6], A.P. Jackson[7,1], G. Bryden[8], N.J. Turner[8], P. Harvey[9], A. Hales[10,11], R.J. De Rosa[12]

概要

- ALMAでTaurusのprotoplanetary diskをsurvey
- disk massを導出し統計的に議論
- low mass star (spectarl type M4 – M7) のサンプルを埋めた

観測と結果

- ALMA Cycle 1, 885 μm continuum (ALMA Band 7)
- samples: Herschelを用いたTBOSS surveyから
  - M type の Class II のみ24天体
  - stellar: M4 – M5 の14天体
    substellar: M6 – M7の10天体
- 空間分解能 ~ 0''.34x0''.24
- 21天体が8σ以上でdetection，J0414+2811のみ5σでdetectionで，計22天体が受かった
- 3σの検出限界は0.27 mJy/beam

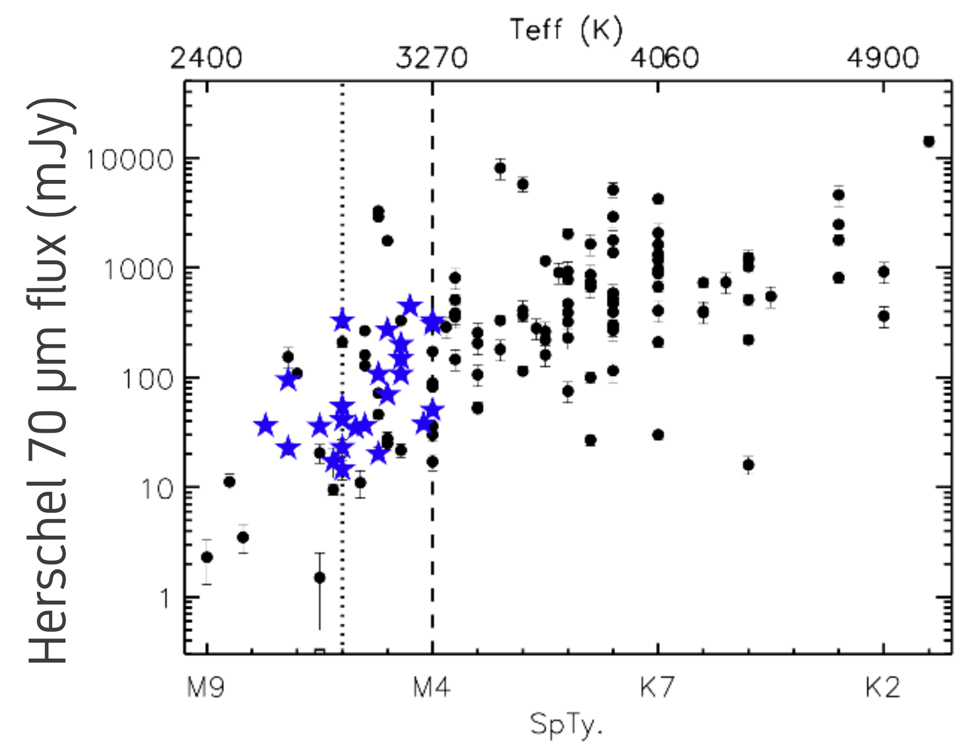

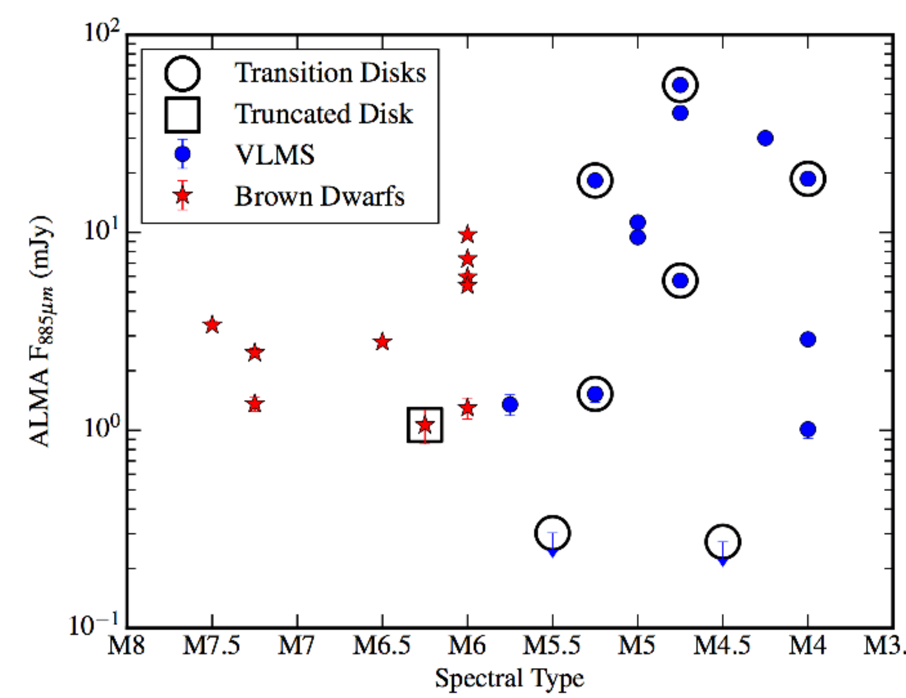

円盤質量の測定

scaling relation

$$\log M_{dust} = \log S_\nu + 2\log d - \log \kappa_\nu - \log B_\nu(\langle T_{dust}\rangle),$$

$$\langle T_{dust}\rangle = A(L_*/L_\odot)^B K$$

- $\kappa_{1.3mm}$ = 2.3 cm^2 g^{-1}, $\kappa_\nu \sim \nu^{0.4}$
- r = 100 au を仮定

→ Mass range~ 0.3–20 M_{earth}

$T_{\rm dust} = A(L_*/L_\odot)^B$

Disk Outer Radius (au)	Amplitude (A)	Index (B)
10	58	0.23
20	41	0.22
40	30	0.18
60	26	0.16
80	24	0.15
100	22	0.15
200	19	0.14

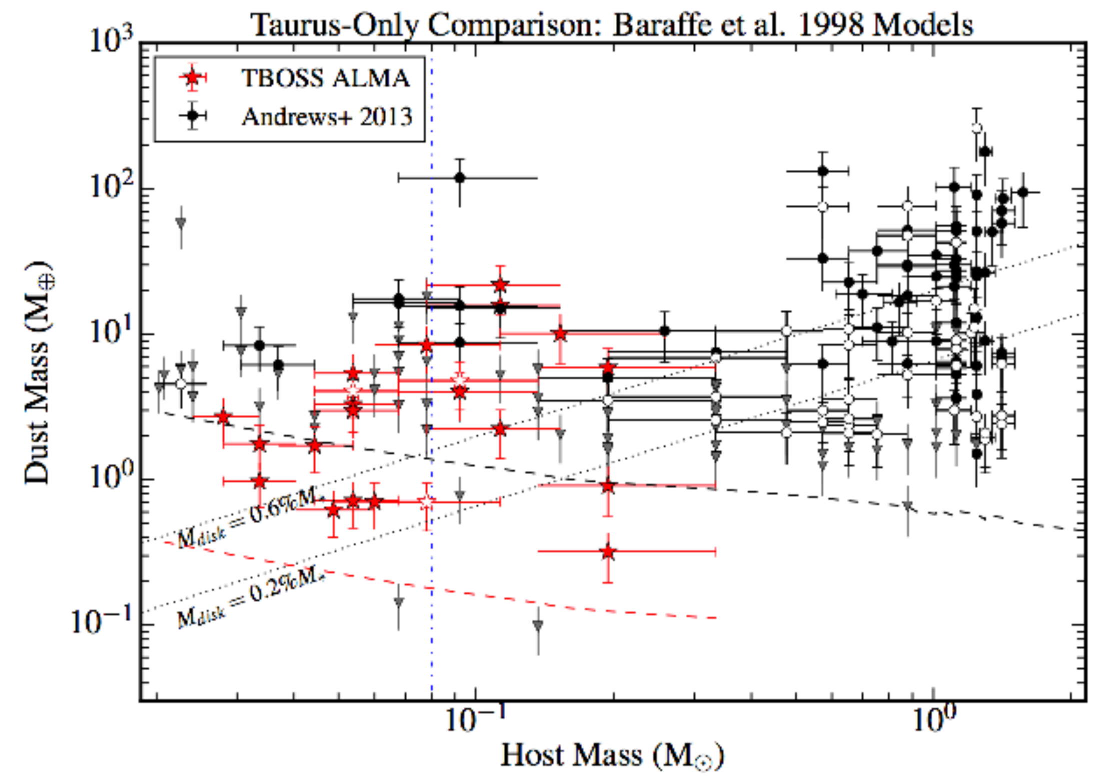

右上がりの傾向

power-law fitting

- M_{dust} vs M_*で正の相関 ($\propto M_*^{0.94\pm0.14}$)
- フィッティング結果はAndrews+13 と一致する結果

→ low mass でも円盤形成プロセスは同じ

- Upper Sco との比較
- slopeはTaurusとほぼ同じ（ $\propto M_*^{0.92\pm0.18}$，ただし恒星進化モデルに依存）
- より進化の進んだUpper Scoではdisk massが減少している

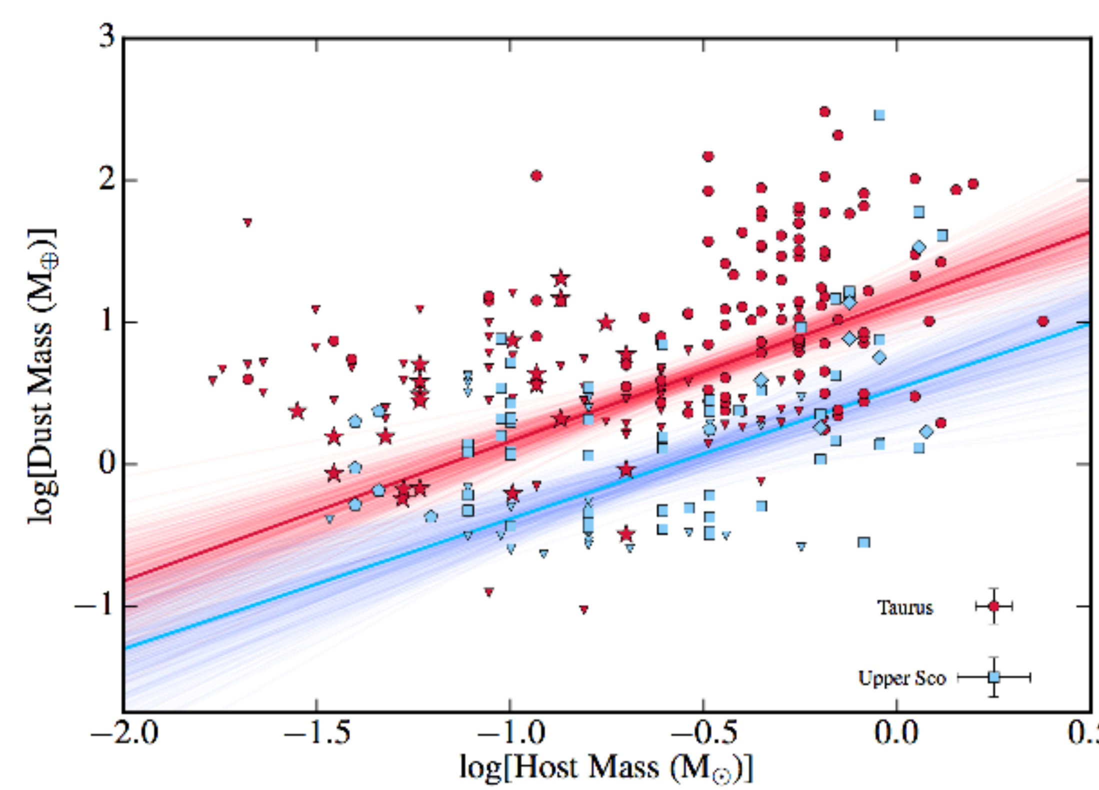

- MMSN gas massを超えるのは24%
- M-star rangeでは17%

↔M-dwarf周囲のgas giantの存在頻度は~2-3 %

→ gas giantを作る効率は低い

- brown dwarf 周りには10M_{earth}を超えるものも少ない

→brown dwarf周りのplanetary mass companionはdisk起源ではない？

- Kepler で見つかった惑星質量をプロット (Mulders+15，惑星周期は2-50 days)
- 見つかった惑星よりもdiskにはもっと質量がある

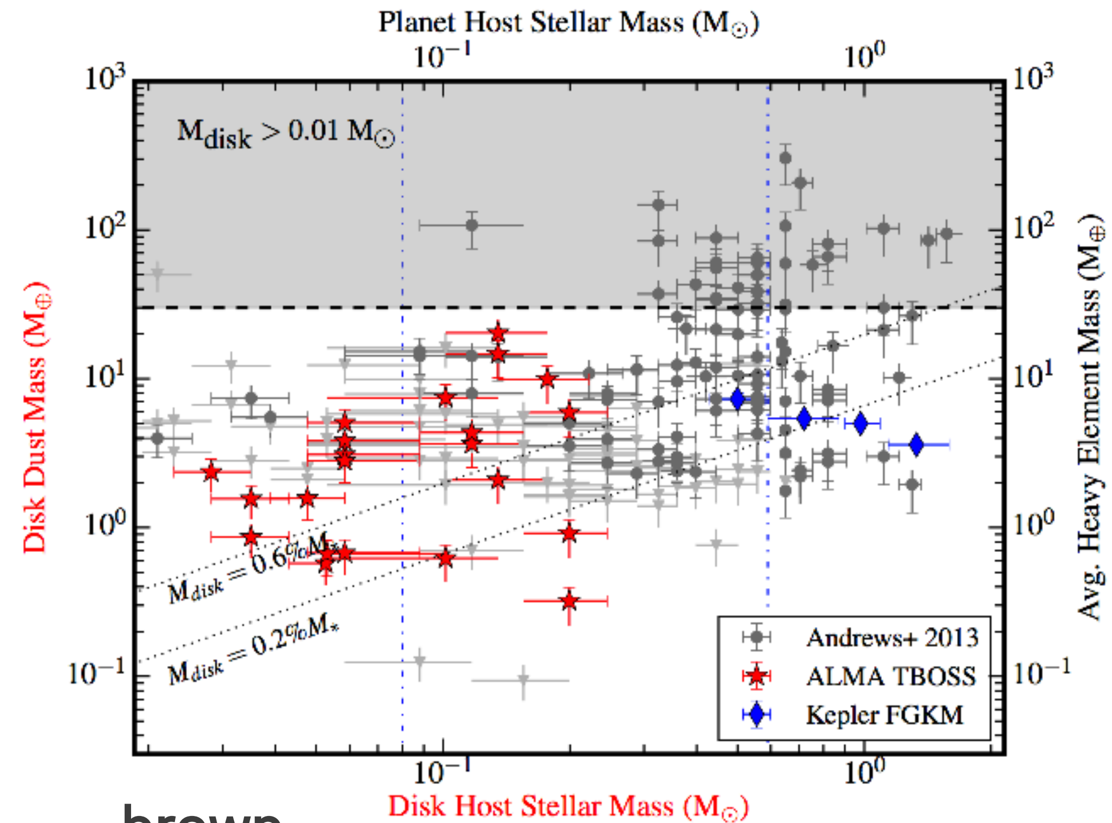

brown dwarf

M-dwarf

- Upper ScoではTaurusと比べてdisk massは減少するが分布は同じ→消えたmassはplanet？
- 惑星形成は1-2 Myr のTaurusから~10 Myr のUpper Scoの間で起こっている

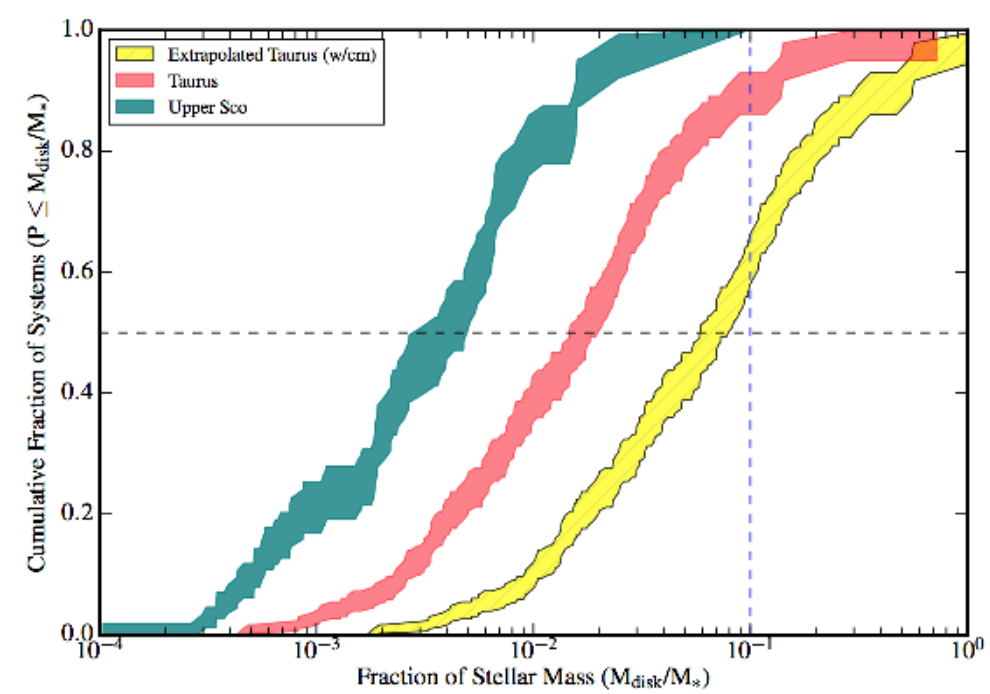

#1 **Similar complex kinematics within two massive, filamentary infrared dark clouds**

A.T. Barnes[1,2,3], J.D. Henshaw[4], P. Caselli[3], I. Jiménez-Serra[5], J.C. Tan[6], F. Fontani[7], A. Pon[8], and S. Ragan[9]

概要

- 大質量形成過程についてよく知りたい
- Infrared dark clouds (IRDCs) の一つである IRDC G034.43+0024 を観測を行った
- IRDC G034.43+0024
  - filament 構造の中に複数の重いcores
  - dense, quiescentなgas
- 速度構造からCloud の形成などを議論

観測

- IRAM 30 m telescope/EMIR
- N2H+ (1-0) と C18O (2-1) 輝線を観測
- それぞれdense core，dense coreよりさらに広がった envelopeをtraceすると期待
- 空間分解能 ~ 0.5 pc

Observational parameter	N_2H^+ (1 – 0)	$C^{18}O$ (1 – 0)
Frequency (MHz)	93176.7637 [a]	109782.1780 [b]
HPBW ($''$) [c]	26	23
Velocity Resolution (km s^{-1})	6.28×10^{-2}	5.33×10^{-2}
Beam Efficiency	0.81	0.78
Forward Efficiency	0.95	0.94
rms (K)	0.13	0.15

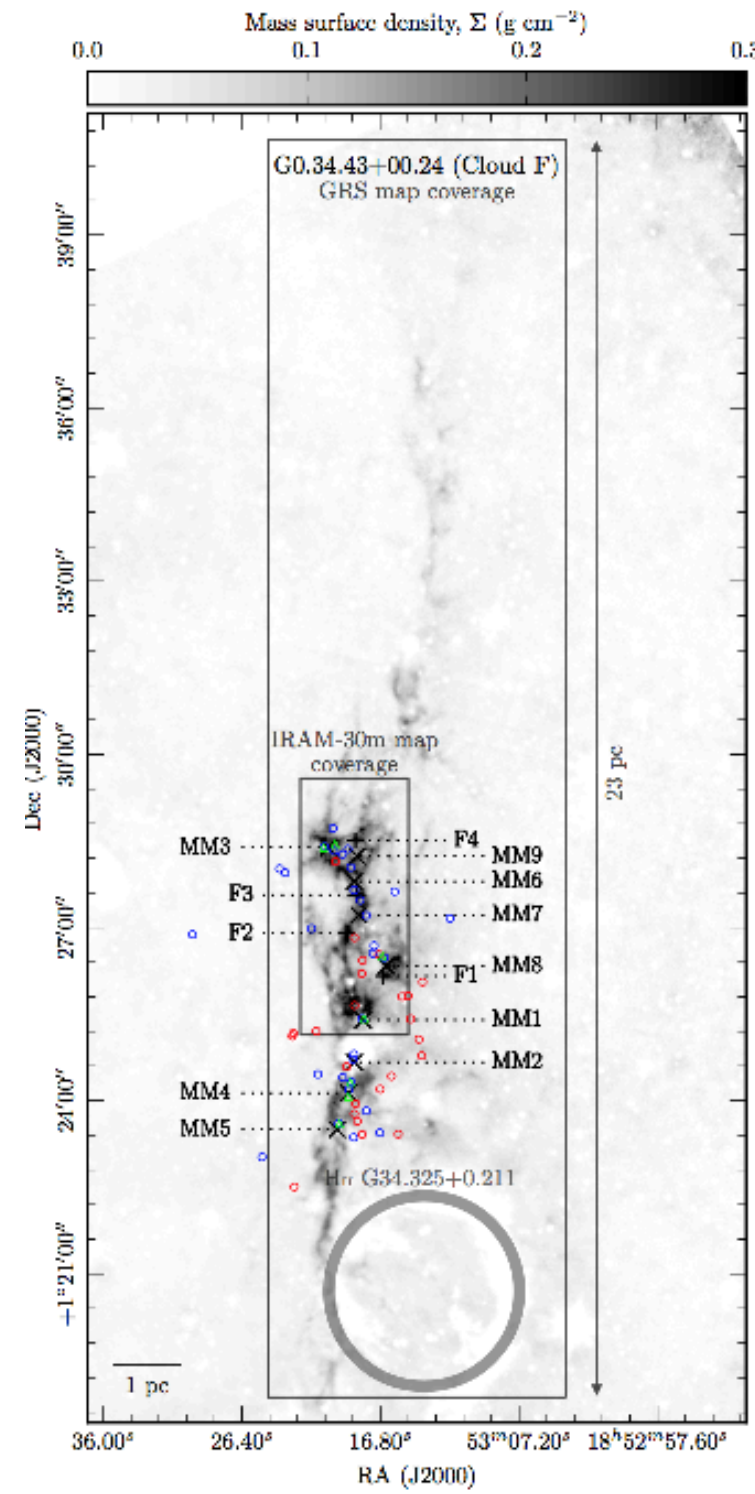

観測結果

surface density　積分強度　速度分布　速度分散

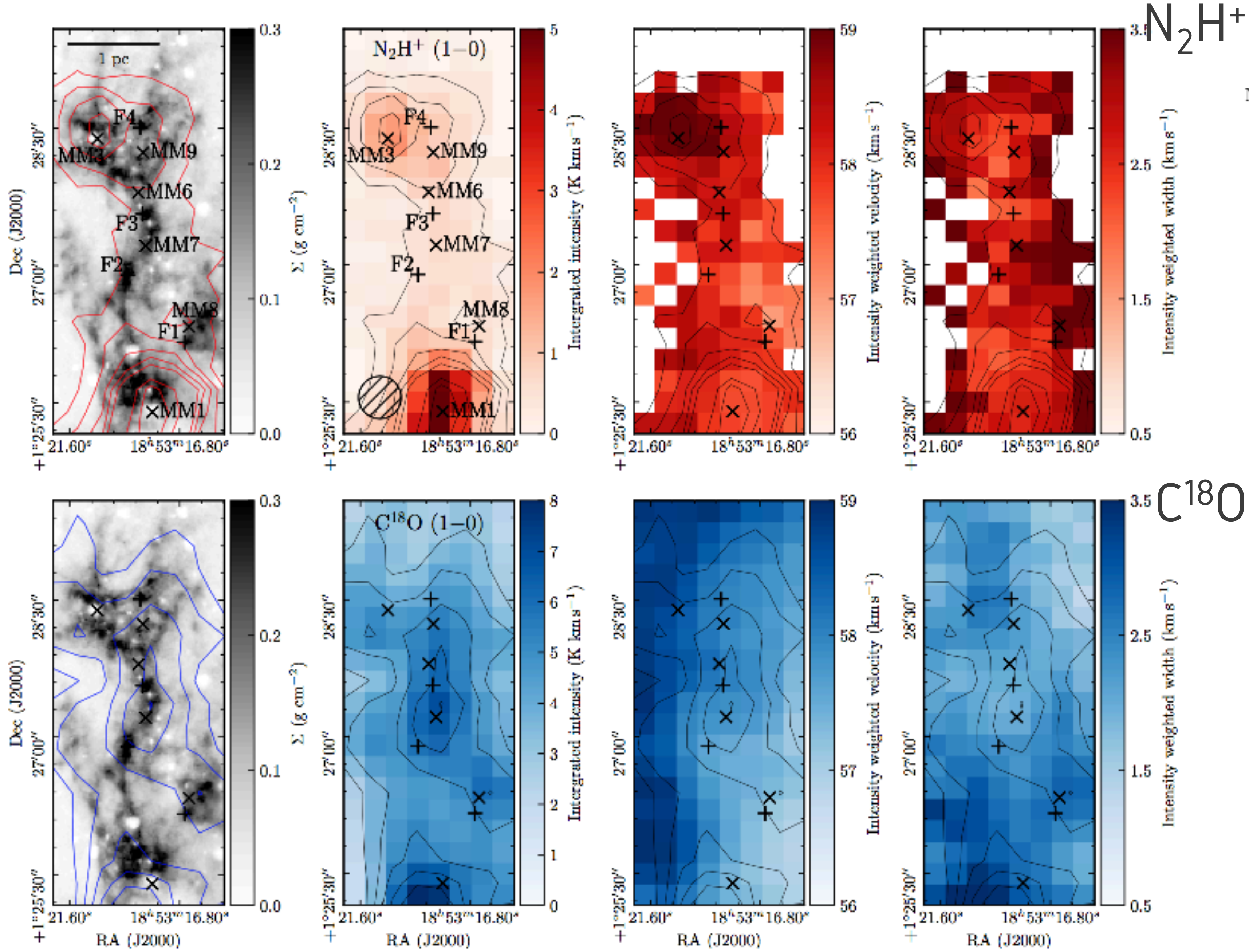

コントア: 積分強度

N2H+　C18O

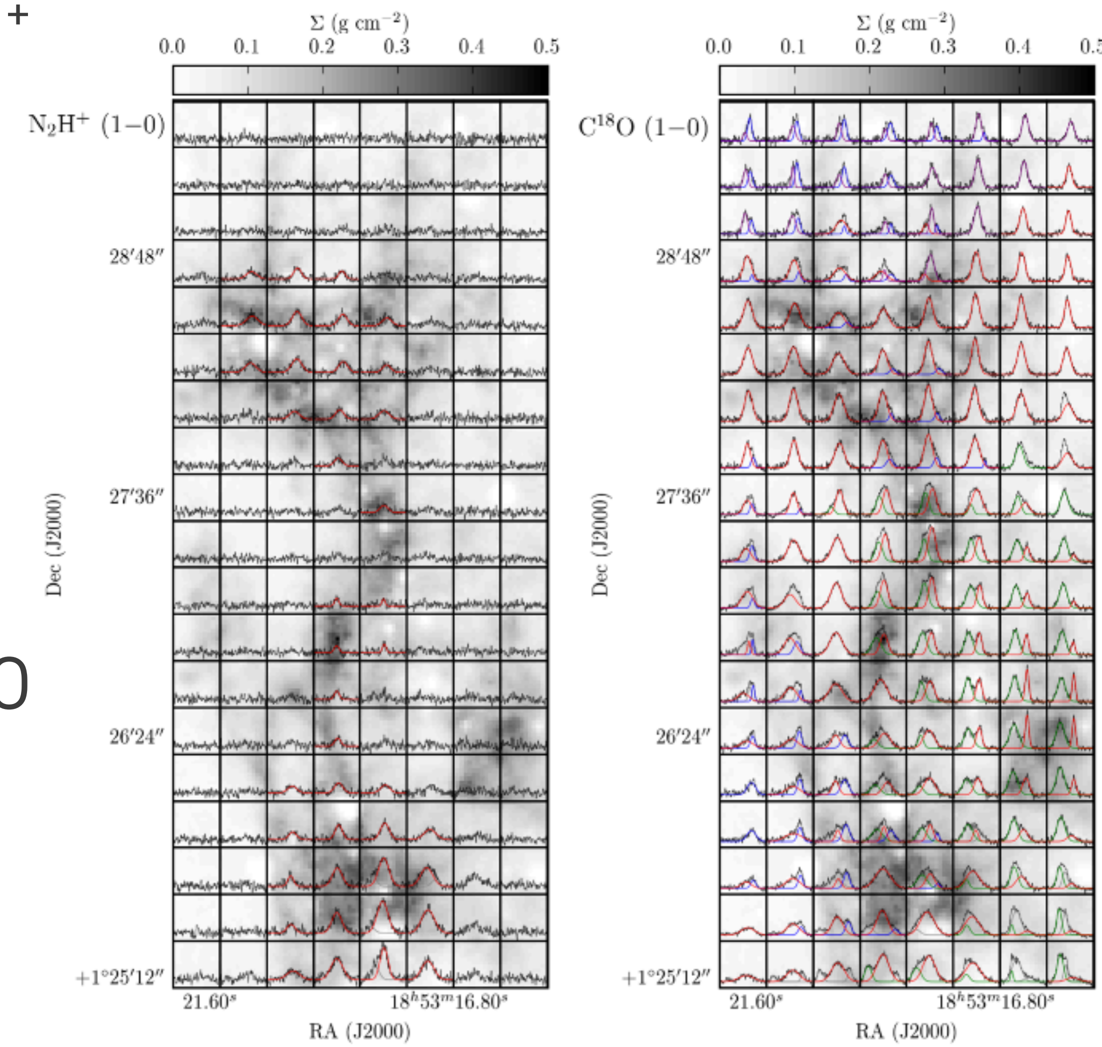

- ピークがいくつかのコアに対応
（MM1, MM3 for N2H+，MM1, MM3, MM7, MM8, F1 for C18O）
- 東西方向に速度勾配
- 速度分散の振る舞いが異なる

- 異なる速度成分を分離する
- semi-automated gaussian fitting

Mapをいくつかに分けた領域 (SAA) で複数のGaussianをfit

- automated hierarchical clustering algorithm

Gaussian fitされた各SAAsの分類を行う

1. 各成分のseparationがbeam size以下
2. 速度差が速度分解能の2倍以下
3. 速度分散の差が0.23 km/s 以下

を満たすなら同じ成分とみなす

Cloud F の速度成分

- N_2H^+は1成分，$C^{18}O$は4成分
- N_2H^+，$C^{18}O$の間で同じ成分F_{PPV4} に速度差

→ $\langle V_{N2H+} - V_{c18o} \rangle$ = +0.32 ± 0.06 km/s

- FPPV1とFPPV2の速度差2.9±0.5 km/s

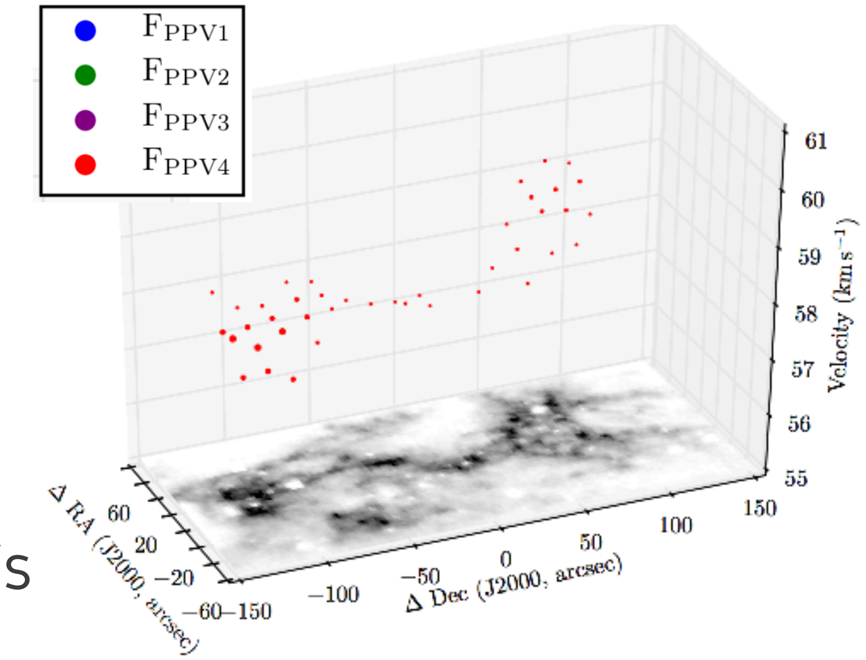

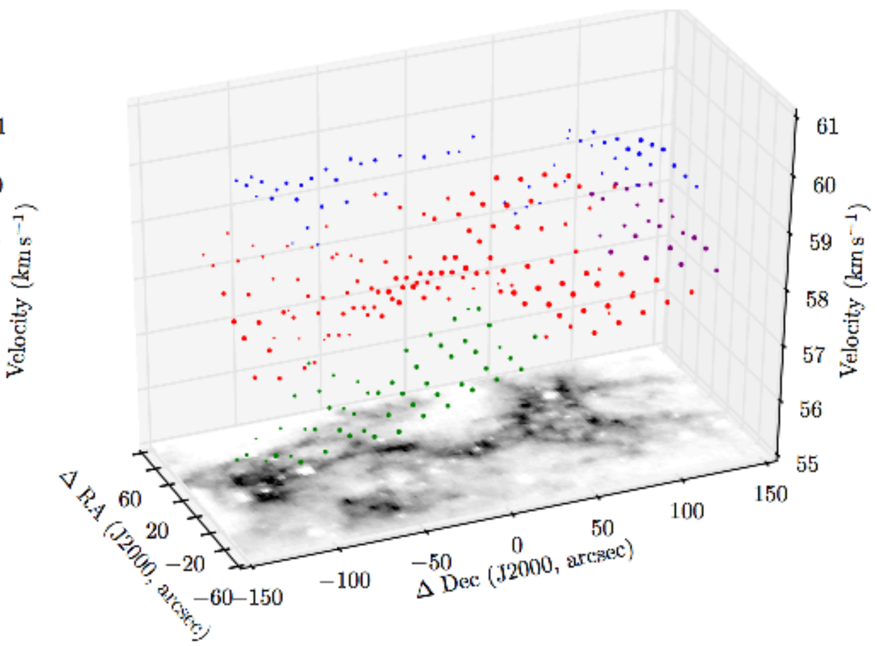

Cloud H (IRDC: G035.39 – 00.33) との比較

- Cloud H にも同じ解析，$C^{18}O$で5成分
- いくつかの共通点
  - 同様の2.9±0.3 km/sの速度差をもつ2成分が存在
  - HPPV4でN_2H^+と$C^{18}O$の間に速度差 +0.26 ± 0.02 km/s

→ 同じ形成シナリオで説明できる？

- Cloud H はfilament merging senario?
  - 高速度の成分 ($H_{PPV1,2}$)と低速度の成分 (H_{PPV3})がmergingして中間速度の成分 (H_{PPV4})が形成
  - N_2H^+は高速度成分に押されたdenseな場所 → $C^{18}O$より高速度になる

Line	Component (colour)	# points	Centroid velocity (V_0) km s^{-1}	Line width (Δv) km s^{-1}	Velocity gradient (∇v) km s^{-1} pc^{-1}	Gradient angle ($\theta_{\nabla v}$) degrees
$C^{18}O$ (1 – 0)						
	F_{PPV1} (blue)	54	59.56 ± 0.24	0.96 ± 0.31	0.12 ± 0.03	-38.89 ± 14.81
	F_{PPV2} (green)	53	56.68 ± 0.40	1.48 ± 0.31	0.25 ± 0.08	-31.07 ± 23.86
	F_{PPV3} (purple)	22	58.39 ± 0.12	1.04 ± 0.27	0.16 ± 0.05	-83.77 ± 4.32
	F_{PPV4} (red)	128	58.26 ± 0.43	1.75 ± 0.60	0.28 ± 0.07	-85.83 ± 5.93
N_2H^+ (1 – 0)						
	F_{PPV4} (red)	41	58.44 ± 0.51	1.75 ± 0.50	0.75 ± 0.15	70.20 ± 3.20
$C^{18}O$ (1 – 0)						
	H_{PPV1} (orange)	20	46.12 ± 0.11	0.47 ± 0.15	0.12 ± 0.06	76.08 ± 12.41
	H_{PPV2} (purple)	27	46.61 ± 0.20	1.39 ± 0.41	0.38 ± 0.11	61.15 ± 9.66
	H_{PPV3} (green)	26	43.67 ± 0.16	1.33 ± 0.38	0.29 ± 0.09	-87.80 ± 7.77
	H_{PPV4a} (red)	21	45.07 ± 0.06	1.48 ± 0.34	0.01 ± 0.02	...
	H_{PPV4b} (blue)	32	45.52 ± 0.25	1.35 ± 0.47	0.33 ± 0.10	-56.27 ± 11.72
N_2H^+ (1 – 0)						
	H_{PPV2} (purple)	14	46.88 ± 0.10	0.74 ± 0.20	0.15 ± 0.08	-29.98 ± 29.89
	H_{PPV4a} (red)	38	45.42 ± 0.10	1.26 ± 0.16	0.02 ± 0.02	...
	H_{PPV4b} (blue)	27	45.99 ± 0.09	1.02 ± 0.35	0.10 ± 0.05	-77.40 ± 10.68

GMC scales for Cloud F

- large scale の観測と今回の観測がよく一致
- Cloud F はより大きなGiant Molecular Filamentの一部の可能性がある

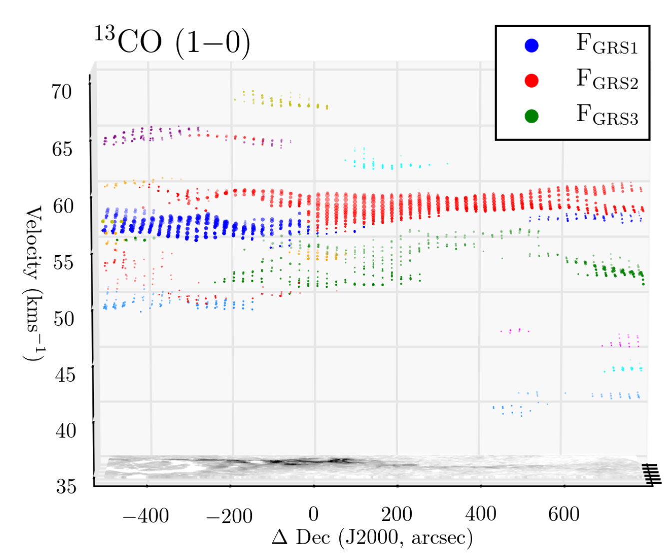

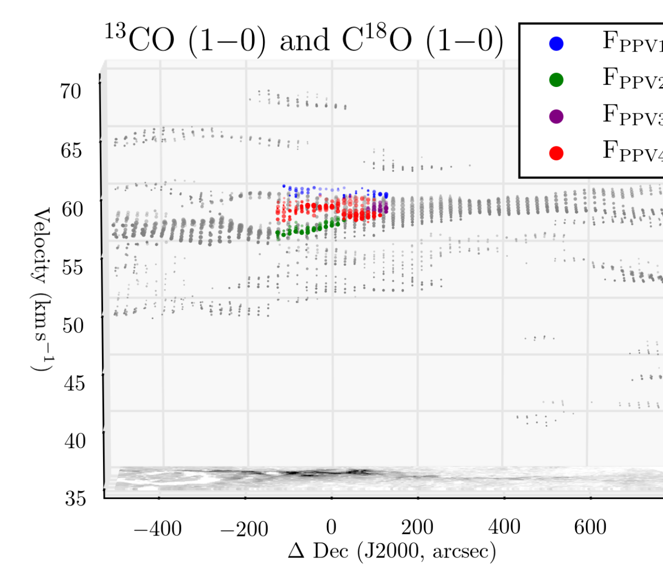

#2

On the diversity and statistical properties of protostellar discs

Matthew R. Bate[1]

概要

- 分子雲から円盤形成の数値シミュレーション
- 初の原始星円盤のpopulation synthesis studyを行なった

計算について

- 3D SPHコードでradiative hydrodynamicsの計算

- 初期条件
  - 一様密度の分子雲
  - 質量: 500 M_{sun}
  - スケール: 0.404 pc
  - 密度: 1.2x10^{-19} g cm^{-3}
  - t_{ff} = 6.0x10^{12} s ~ 1.90x10^5 yr
  - T = 10.3 K
  - 乱流あり（rms: M=13.7）
- 円盤の条件
  - r < 2000 au かつ軌道の離心率e < 0.3のSPH粒子
  - 次のものは除外
    - M_{disk} < 0.003 M_{sun} 以下，全円盤質量の63%を含む半径が300 au以上，63%を含む半径が50%を含む半径の3倍以上
  - 円盤半径
    - 全円盤質量の63.2%を含む半径

$$\Sigma(r) = \Sigma_c \left(\frac{r}{r_c}\right)^{-\gamma} \exp\left[-\left(\frac{r}{r_c}\right)^{(2-\gamma)}\right],$$

- 計算は1.20 t_{ff} ~ 0.23 Myr まで
- 最も進化した protostar は 0.9x10^5 yr
- 分解能は円盤サイズ 10 au
- 最終的に 84のsingle protostarと40のmultiple systems（28 binary, 5 triple, 7 quadruple）が形成

結果

多様な円盤

- misaligned systems, spiral, warped disks, etc.
- 典型的に
  - $M_* \sim 0.02 - 0.4\ M_{sun}$
  - $M_{disk} \sim 0.003 - 0.5\ M_{sun}$
  - $R_{disk} \sim 20 - 100$ au

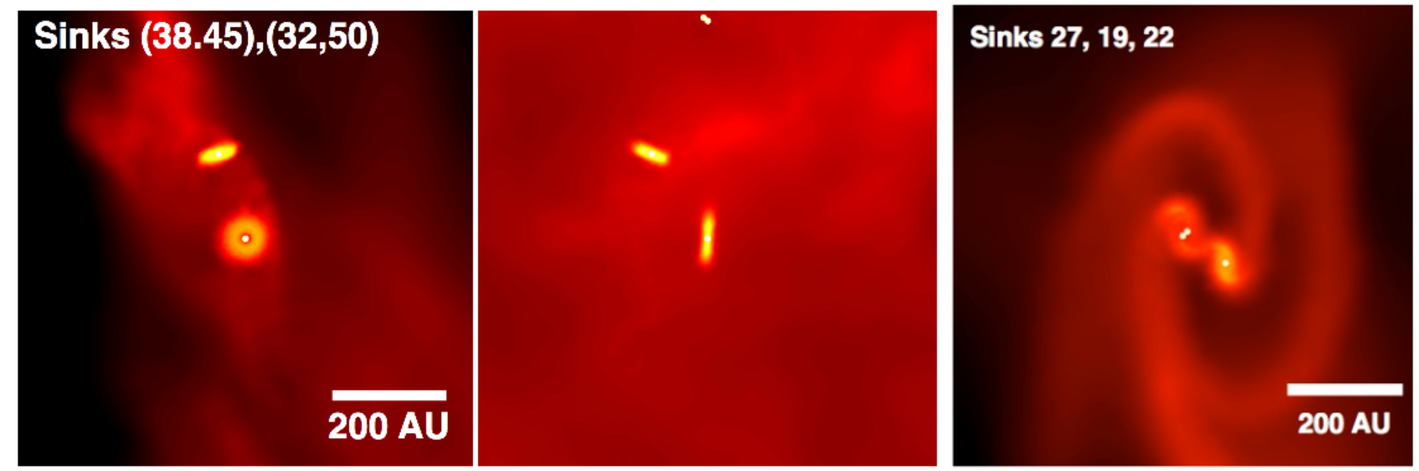

all systems

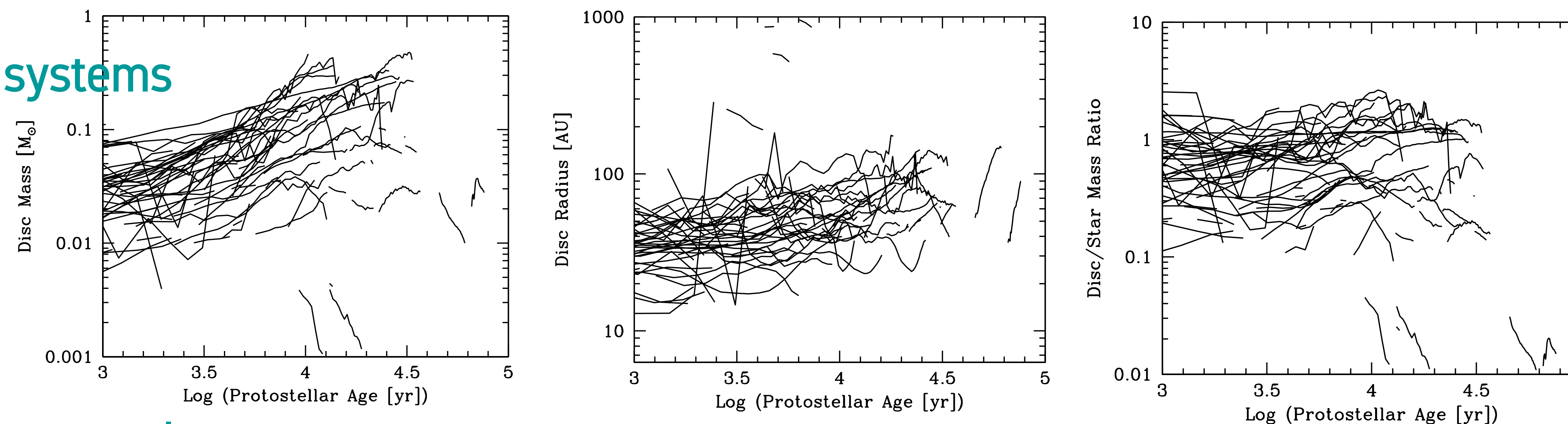

No encounters

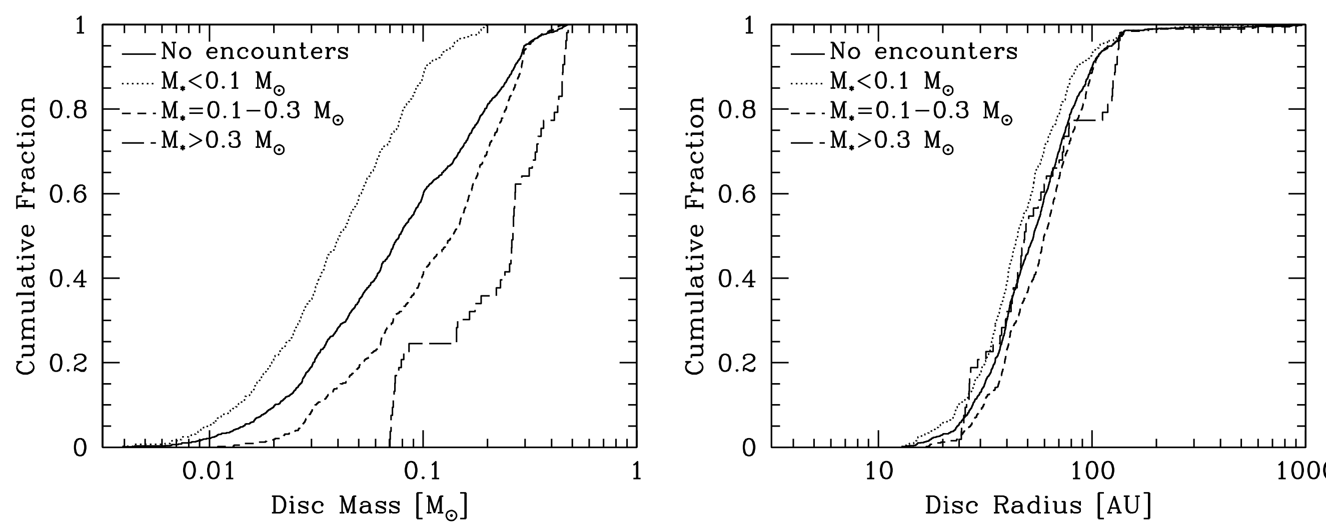

disk mass

- 時間とともに増加
- 典型的に10^3 yr – 10^4 yrで3倍程度まで成長
- 10^4 yrより先はdisk massが減少
- $M_d \propto M_*$~0.85 ($M_* < 0.5\ M_{sun}$)

disk radii

- rc $\propto$ M*~0.25
- M* < 0.1 Msunでrc=20をきる小さな円盤は~ 50 %
- M*>0.3 Msunでは ~ 10 %

disk/stellar mass ratio

- Md/M* ~ 0.1 -2
- 時間によらず一定
- M* 0.1 – 0.3 で高い傾向

pair のdisks，軌道,中心星spinのaligenment

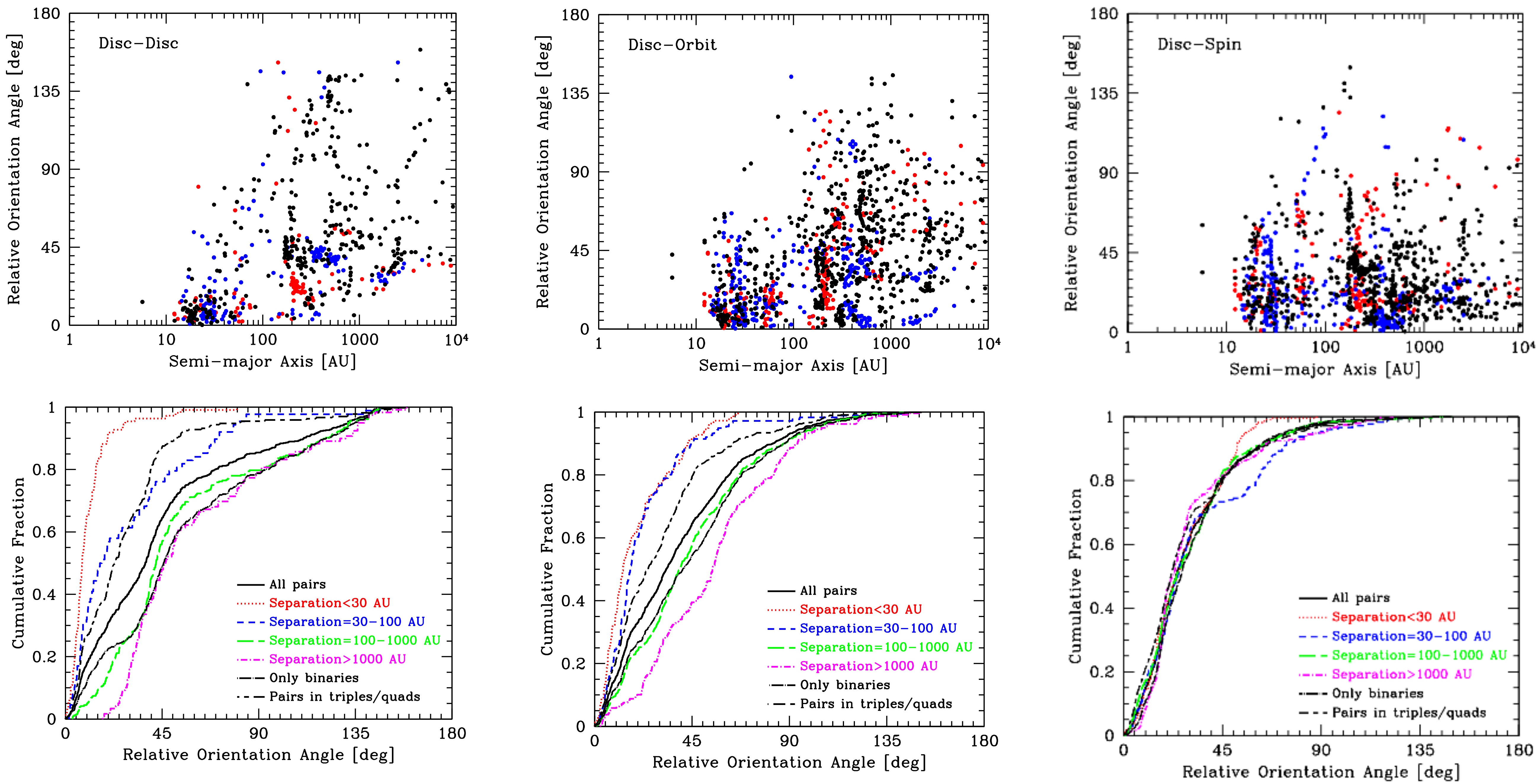

それぞれのcircumstellar diskはpairのseparationが大きいほどmisaligned

pairのseparationが大きいほど強くmisaligned

separationに関係なく50%ほどのpairで円盤とspinがmisaligned

観測との比較

vs Class II disks

- disk mass: ~ 10^4 yrの若いdiskの方がClass IIのdiskに比べて30 – 300倍重い
- disk radius: 分布は観測とシミュレーションでよく一致

dust mass

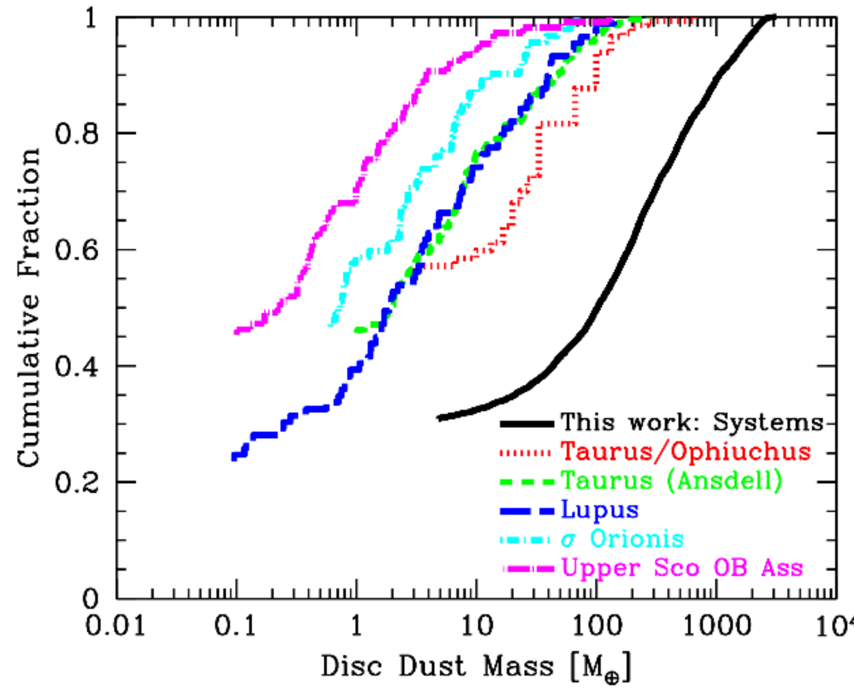

The observational surveys are of Taurus/Ophiuchus (Andrews & Williams 2007), the reanalysis of Taurus data (Andrews et al. 2013) by (Ansdell et al. 2016), Lupus (Ansdell et al. 2016), σ Orionis (Ansdell et al. 2017), and the Upper Scorpius OB association (Barenfeld et al. 2016). As may be ex-

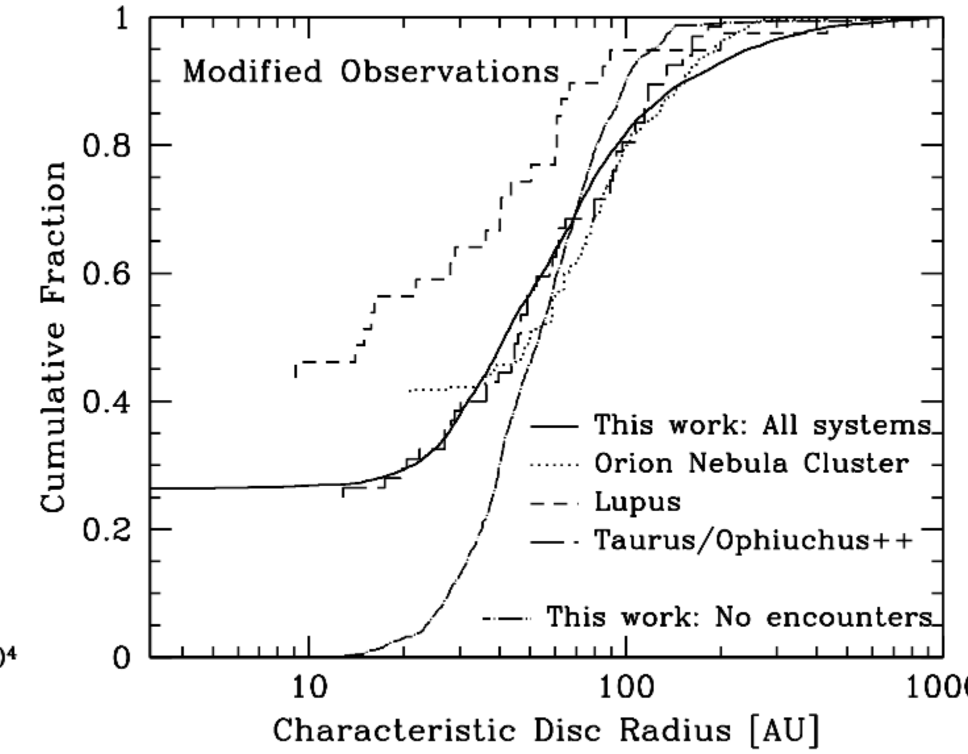

the Orion Nebula Cluster (Vicente & Alves 2005), Lupus (Tazzari et al. 2017), a sample of discs in Taurus, Ophiuchus, and other regions (Tripathi et al. 2017), and Ophiuchus (Andrews et al. 2009, 2010).

vs Class 0 disks

- disk mass: 観測から0.05 – 0.2 M_{sun} (Jorgensen+9, Enoch+11), 0.09 - 0.36 M_{sun} (Segura-Cox+16)
- シミュレーション（0.02 - 0.4 M_{sun}）とコンシステント
- disk radius も比較的コンシステント

gas mass

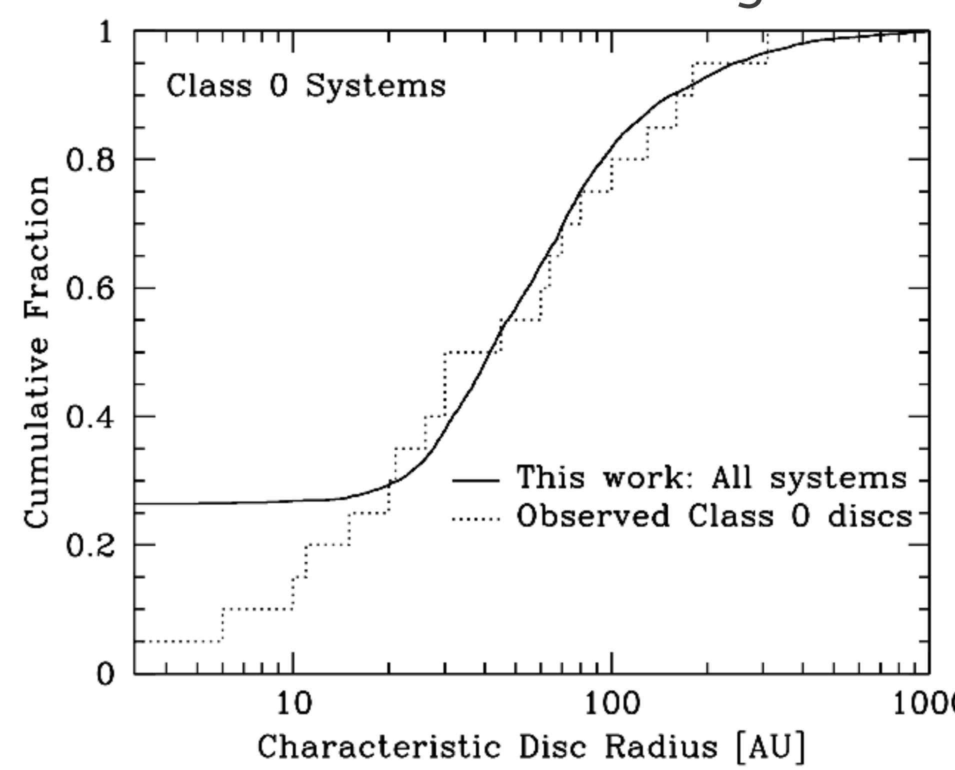

- disk mass は disk radiusにはあまり依らない
- Class 0からClass IIへはdisk radiusを保ったまま質量のみを減らして進化する

Spatially associated clump populations in Rosette from CO and dust maps

Todor V. Veltchev[1,2], Volker Ossenkopf-Okada[3], Orlin Stanchev[1], Nicola Schneider[3], Sava Donkov[4], and Ralf S. Klessen[2]

[1] University of Sofia, Faculty of Physics, 5 James Bourchier Blvd., 1164 Sofia, Bulgaria; [2] Universität Heidelberg, Zentrum für Astronomie, Institut für Theoretische Astrophysik, Albert-Ueberle-Str. 2, 69120 Heidelberg, Germany; [3] I. Physik. Institut, University of Cologne, D-50937 Cologne, Germany; [4] Department of Applied Physics, Technical University, 8 Kliment Ohridski Blvd., 1000 Sofia, Bulgaria

E-mail contact: eirene *at* phys.uni-sofia.bg

Spatial association of clumps from different tracers turns out to be a valuable tool to determine the physical properties of molecular clouds. It provides a reliable estimate for the X-factors, serves to trace the density of clumps seen in column densities only and allows to measure the velocity dispersion of clumps identified in dust emission. We study the spatial association between clump populations, extracted by use of the GAUSSCLUMPS technique from ^{12}CO (1–0), ^{13}CO (1–0) line maps and Herschel dust-emission maps of the star-forming region Rosette, and analyse their physical properties. All CO clumps that overlap with another CO or dust counterpart are found to be gravitationally bound and located in the massive star-forming filaments of the molecular cloud. They obey a single mass-size relation $M_{\rm cl} \propto R_{\rm cl}^{\gamma}$ with $\gamma = 3$ (implying constant mean density) and display virtually no velocity-size relation. We interpret their population as low-density structures formed through compression by converging flows and still not evolved under the influence of self-gravity. The high-mass parts of their clump mass functions are fitted by a power law $dN_{\rm c}l/d\log M_{\rm cl} \propto M_{\rm cl}^{\Gamma}$ and display a nearly Salpeter slope $\Gamma \sim -1.3$. On the other hand, clumps extracted from the dust-emission map exhibit a shallower mass-size relation with $\gamma = 2.5$ and mass functions with very steep slopes $\Gamma \sim -2.3$ even if associated with CO clumps. They trace density peaks of the associated CO clumps at scales of a few tenths of pc where no single density scaling law should be expected.

Accepted by MNRAS

Radiation Transfer of Models of Massive Star Formation. IV. The Model Grid and Spectral Energy Distribution Fitting

Yichen Zhang[1] and Jonathan C. Tan[2,3]

[1] The Institute of Physical and Chemical Research (RIKEN), Hirosawa 2-1, Wakoshi, Saitama, Japan; [2] Department of Astronomy, University of Florida, Gainesville, FL 32611, USA; [3] Department of Physics, University of Florida, Gainesville, FL 32611, USA

E-mail contact: yczhang.astro *at* gmail.com

We present a continuum radiative transfer model grid for fitting observed spectral energy distributions (SEDs) of massive protostars. The model grid is based on the paradigm of core accretion theory for massive star formation with pre-assembled gravitationally-bound cores as initial conditions. In particular, following the Turbulent Core Model, initial core properties are set primarily by their mass and the pressure of their ambient clump. We then model the evolution of the protostar and its surround structures in a self-consistent way. The model grid contains about 9000 SEDs with 4 free parameters: initial core mass, the mean surface density of the environment, the protostellar mass, and the inclination. The model grid is used to fit observed SEDs via χ^2 minimization, with the foreground extinction additionally estimated. We demonstrate the fitting process and results using the example of massive protostar G35.20-0.74. Compared with other SED model grids currently used for massive star formation studies, in our model grid, the properties of the protostar and its surrounding structures are more physically connected, which reduces the dimensionality of the parameter spaces and the total number of models. This excludes possible fitting of models that are physically unrealistic or that are not internally self-consistent in the context of the Turbulent Core Model. Thus, this model grid serves not only as a fitting tool to estimate properties of massive protostars, but also as a test of core accretion theory. The SED model grid is publicly released with this paper.

Accepted by ApJ

Magnetic fields at the onset of high-mass star formation

Henrik Beuther[1], Juan Soler[1], Wouter Vlemmigs[2], Hendrik Linz[1], Thomas Henning[1], Rolf Kuiper[3], Ram Rao[4], Rowan Smith[5], Takeshi Sakai[6], Katharine Johnston[7], Andrew Walsh[8] and Siyi Feng[9]

[1] Max Planck Institute for Astronomy, Koenigstuhl 17, 69117 Heidelberg, Germany; [2] Department of Earth and Space Sciences Chalmers University of Technology, Onsala Space Observatory, 439 92, Onsala, Sweden; [3] Institute of Astronomy and Astrophysics, University of Tuebingen, Auf der Morgenstelle 10, 72076, Tuebingen, Germany; [4] Academia Sinica Institute of Astronomy and Astrophysics, 645 N. Aohoku Place, Hilo, HI 96720, USA 0000-0002-1407-7944; [5] School of Physics and Astronomy, University of Manchester, Oxford Road, Manchester M13 9PL, UK; [6] Department of Communication Engineering and Informatics, The University of Electro-Communications, Chofugaoka, Chofu, Tokyo 182-8585, Japan; [7] School of Physics and Astronomy, University of Leeds, Leeds, LS2 9JT, UK; [8] International Centre for Radio Astronomy Research, Curtin University, GPO Box U1987, Perth WA 6845, Australia; [9] Max-Planck-Institut fuer Extraterrestrische Physik, Giessenbachstrasse 1, 85748 Garching, Germany

E-mail contact: beuther *at* mpia.de

Context: The importance of magnetic fields at the onset of star formation related to the early fragmentation and collapse processes is largely unexplored today.
Aims: We want to understand the magnetic field properties at the earliest evolutionary stages of high-mass star formation.
Methods: The Atacama Large Millimeter Array is used at 1.3 mm wavelength in full polarization mode to study the polarized emission and by that the magnetic field morphologies and strengths of the high-mass starless region IRDC 18310-4.
Results: The polarized emission is clearly detected in four sub-cores of the region. In general it shows a smooth distribution, also along elongated cores. Estimating the magnetic field strength via the Davis-Chandrasekhar-Fermi method and following a structure function analysis, we find comparably large magnetic field strengths between $\sim$0.6 and 3.7 mG. Comparing the data to spectral line observations, the turbulent-to-magnetic energy ratio is low, indicating that turbulence does not significantly contribute to the stability of the gas clump. A mass-to-flux ratio around the critical value 1.0 – depending on column density – indicates that the region starts to collapse which is consistent with the previous spectral line analysis of the region.
Conclusions: While this high-mass region is collapsing and thus at the verge of star formation, the high magnetic field values and the smooth spatial structure indicate that the magnetic field is important for the fragmentation and collapse process. This single case study can only be the starting point for larger sample studies of magnetic fields at the onset of star formation.

Accepted by Astronomy & Astrophysics

K2 REVEALS PULSED ACCRETION DRIVEN BY THE 2 MYR OLD HOT JUPITER CI TAU B

LAUREN I. BIDDLE,[1,2] CHRISTOPHER M. JOHNS-KRULL,[3] JOE LLAMA,[1] LISA PRATO,[1] AND BRIAN A. SKIFF[1]

[1] *Lowell Observatory, 1400 W. Mars Hill Rd. Flagstaff. Arizona. 86001. USA.*
[2] *Department of Physics & Astronomy, Northern Arizona University, 527 S. Beaver St. Flagstaff. Arizona. 86011. USA.*
[3] *Department of Physics & Astronomy, Rice University, 6100 Main St. MS-108, Houston, TX 77005*

(Accepted for publication in ApJ Letters)

ABSTRACT

CI Tau is a young (~2 Myr) classical T Tauri star located in the Taurus star forming region. Radial velocity observations indicate it hosts a Jupiter-sized planet with an orbital period of approximately 9 days. In this work, we analyze time series of CI Tau's photometric variability as seen by *K2* . The lightcurve reveals the stellar rotation period to be ~6.6 d. Although there is no evidence that CI Tau b transits the host star, a ~9 d signature is also present in the lightcurve. We believe this is most likely caused by planet-disk interactions which perturb the accretion flow onto the star, resulting in a periodic modulation of the brightness with the ~ 9 d period of the planet's orbit.

Keywords: stars: individual (CI Tau) – stars: activity – stars: magnetic field – stars: planet-disk interactions

5

Pebble isolation mass — scaling law and implications for the formation of super-Earths and gas giants

Bertram Bitsch[1], Alessandro Morbidelli[2], Anders Johansen[1], Elena Lega[2], Michiel Lambrechts[1], and Aurélien Crida[2,3]

[1] Lund Observatory, Department of Astronomy and Theoretical Physics, Lund University, 22100 Lund, Sweden; [2] University Nice-Sophia Antipolis, CNRS, Observatoire de la Cote d'Azur, Laboratoire LAGRANGE, CS 34229, 06304 Nice cedex 4, France; [3] Institut Universitaire de France, 103 Boulevard Saint-Michel, 75005 Paris, France

E-mail contact: bert *at* astro.lu.se

The growth of a planetary core by pebble accretion stops at the so called pebble isolation mass, when the core generates a pressure bump that traps drifting pebbles outside its orbit. If the isolation mass is very small, then gas accretion is protracted and the planet remains at a few Earth masses with a mainly solid composition. For larger values of the pebble isolation mass, the planet might be able to accrete gas from the protoplanetary disc and grow into a gas giant. Previous works have determined a scaling of the pebble isolation mass with cube of the disc aspect ratio. Here we expand on previous measurements and explore the dependency of the pebble isolation mass on all relevant parameters of the protoplanetary disc. We use 3D hydrodynamical simulations to measure the pebble isolation mass and derive a simple scaling law that captures the dependence on the local disc structure and the turbulent viscosity parameter α. We find that small pebbles, coupled to the gas, with Stokes number $\tau_f < 0.005$ can drift through the partial gap at pebble isolation mass. However, as the planetary mass increases, particles must be decreasingly smaller to penetrate through the pressure bump. Turbulent diffusion of particles, however, can lead to an increase of the pebble isolation mass by a factor of two, depending on the strength of the background viscosity and on the pebble size. We finally explore the implications of the new scaling law of the pebble isolation mass on the formation of planetary systems by numerically integrating the growth and migration pathways of planets in evolving protoplanetary discs. Compared to models neglecting the dependence of the pebble isolation mass on the -viscosity, our models including this effect result in larger core masses for giant planets. These larger core masses are more akin to the core masses of the giant planets in the Solar System.

Accepted by A&A